Unbalanced collagenases/TIMP-1 expression and epithelial apoptosis in experimental lung fibrosis

Victor Ruiz, Rosa Ma. Ordóñez, Jaime Berumen, Remedios Ramírez, Bruce Uhal, Carina Becerril, Annie Pardo and Moisés Selman

Am J Physiol Lung Cell Mol Physiol 285:L1026-L1036, 2003. First published 25 July 2003; doi:10.1152/ajplung.00183.2003

AJP - Lung Cellular and Molecular Physiology publishes original research covering the broad scope of molecular, cellular, and integrative aspects of normal and abnormal function of cells and components of the respiratory system. It is published 12 times a year (monthly) by the American Physiological Society, 9650 Rockville Pike, Bethesda MD 20814-3991. ISSN: 1040-0605, ESSN: 1522-1504. Visit our website at http://www.the-aps.org/.

Am J Physiol Lung Cell Mol Physiol 285: L1026–L1036, 2003.
First published July 25, 2003; 10.1152/ajplung.00183.2003.

Unbalanced collagenases/TIMP-1 expression and epithelial apoptosis in experimental lung fibrosis

Victor Ruiz,[1] Rosa Ma. Ordóñez,[2] Jaime Berumen,[2] Remedios Ramírez,[3] Bruce Uhal,[4] Carina Becerril,[1] Annie Pardo,[3] and Moisés Selman[1]

[1]*Instituto Nacional de Enfermedades Respiratorias, Mexico City, CP14080,* [2]*Hospital General de Mexico, SSA, Mexico City, CP06720, and* [3]*Facultad de Ciencias, Universidad Nacional Autónoma de Mexico, Mexico City, CP04510, Mexico; and* [4]*Department of Physiology, Michigan State University, Lansing, Michigan 48824*

Submitted 9 June 2003; accepted in final form 20 July 2003

Ruiz, Victor, Rosa Ma. Ordóñez, Jaime Berumen, Remedios Ramírez, Bruce Uhal, Carina Becerril, Annie Pardo, and Moisés Selman. Unbalanced collagenases/TIMP-1 expression and epithelial apoptosis in experimental lung fibrosis. *Am J Physiol Lung Cell Mol Physiol* 285: L1026–L1036, 2003. First published July 25, 2003; 10.1152/ajplung.00183.2003.—In this study, we examined the sequential expression of several matrix metalloproteinases (MMPs), tissue inhibitors of metalloproteinases (TIMPs), and growth factors as well as the presence of apoptosis in a model of pulmonary fibrosis induced in rats with paraquat and hyperoxia. Animals showing neither clinical nor morphological changes with this double aggression were classified as "resistant". Rats were killed at 1, 2, 3, and 6 wk, and lungs were used for collagen content, gene expression by real-time PCR, gelatinolytic activity by zymography, apoptosis by in situ DNA fragmentation, and protein localization by immunohistochemistry. Our results showed a significant decrease of collagenases MMP-8 and MMP-13, with an increase of TIMP-1 and transforming growth factor-β. Immunoreactive TIMP-1 was increased in experimental rats and primarily localized in alveolar macrophages. Expression of gelatinases MMP-2 and MMP-9 mRNAs was not affected, but lung zymography revealed an increase in progelatinase B, progelatinase A, and its active form. Epithelial apoptosis was evident from the first week, whereas at later periods, interstitial cell apoptosis was also noticed. Resistant animals behave as controls. These findings suggest that an imbalance between collagenases and TIMPs, excessive gelatinolytic activity, and epithelial apoptosis participate in the fibrotic response in this experimental model.

gelatinases; tissue inhibitor of metalloproteinases-1

PULMONARY FIBROSIS is the final result of many severe lung injuries, and it is characterized by an initial diffuse inflammatory reaction or epithelial injury/activation followed by fibroblast/myofibroblast proliferation and extracellular matrix accumulation (34). The molecular mechanisms involved in the extensive structural disorganization/remodeling that characterize the fibrotic response are not completely understood but probably involve disequilibrium of some matrix metalloproteinases (MMPs) and tissue inhibitors of metalloproteinases (TIMPs) (33, 36, 45).

The MMP family consists of 23 human enzymes that collectively degrade extracellular matrix components and exert selective proteolysis of cell surface receptors, adhesion molecules, chemokines, cytokines, and growth factors (28, 30, 58). Human MMPs have been classified into six different subgroups of closely related members with rather distinctive but often overlapping substrate specificities: collagenases, gelatinases, stromelysins, matrilysins, membrane type MMPs, and other MMPs. Collagenases (MMP-1, MMP-8, and MMP-13) degrade mainly fibrillar collagens, whereas gelatinases (MMP-2 and MMP-9) have, among others, substrate affinity for basement membrane type IV collagen. The TIMP family is composed of four members (-1, -2, -3, and -4) that bind to the active site of MMPs. In addition to their inhibitory effects on MMPs, some of them show other properties, such as association with latent MMPs, cell growth-promoting activity, cell survival-promoting activity, and apoptosis (3, 15, 16, 29, 58).

Importantly, modifications in MMP and TIMP expression or activity may participate in not only enhancing the exaggerated accumulation of extracellular matrix, but also through the disruption of the basement membranes that seems to play a role in lung fibrogenesis (13, 33, 39, 42). MMPs and TIMPs are regulated by a number of growth factors. Transforming growth factor (TGF)-β inhibits MMP-1 and stimulates TIMP-1 production (19, 27, 38). Its downstream gene transcriptional activity includes an increase in connective tissue growth factor (CTGF) (49). Other important profibrotic or matrix modulating genes are platelet-derived growth factor (PDGF) and angiotensin, which have also been implicated in human and/or experimental fibrosis (2, 9, 24, 46).

On the other hand, a considerable body of literature suggests that the integrity of the alveolar epithelium and alveolar apoptosis is a critical determinant in the pathways that initiate fibrogenesis in the lung (1, 11, 17, 18, 20, 51, 52). Alveolar epithelial cells express functional Fas, and activation of Fas in vivo induces epithelial cell apoptosis and lung fibrosis in mice (11, 17, 18). Likewise, fibroblasts from human fibrotic lungs

Address for reprint requests and other correspondence: M. Selman, Instituto Nacional de Enfermedades Respiratorias, Tlalpan 4502, Col. Sección XVI, México DF, CP 14080, México (E-mail: mselman@sni.conacyt.mx).

The costs of publication of this article were defrayed in part by the payment of page charges. The article must therefore be hereby marked "*advertisement*" in accordance with 18 U.S.C. Section 1734 solely to indicate this fact.

induce epithelial apoptosis, and fibroblastic foci are usually found close to abnormal or denuded alveolar epithelium (51, 52).

With these precedents, our aims were: *1*) to determine the sequential expression of MMP-8 and MMP-13 (collagenases-2 and -3), MMP-2 and MMP-9 (gelatinases A and B), TIMP-1, -2, and -3, TGF-β1, CTGF, angiotensin, and PDGF-A in an established rat model of pulmonary fibrosis, and *2*) to define the timing and location of cell apoptosis. We report here that progression to fibrosis is characterized by decreased expression of MMP-8 and MMP-13, with increased expression of TIMP-1 and TGF-β1, and persistent alveolar epithelial apoptosis.

MATERIALS AND METHODS

Experimental model. The experimental model of diffuse pulmonary fibrosis was developed in rats as described previously (7, 44). Wistar male and female rats were obtained from the same source at the same time and reproduced in our animal facility by the simple rotation method of breeding. Because the Wistar rat is an outbreed strain, we used a breeding system known as "minimum inbreeding for the bred" (4). Adult rats, weighing 200–250 g, received 2.5 mg/kg of paraquat (1,1′-dimethyl-4,4′-bipyridinium; Sigma Chemical, St. Louis, MO) twice weekly for 6 wk through intraperitoneal injections. During all 6 wk, rats were placed into a 160-liter Plexiglas exposure chamber that was continuously ventilated with a mixture of oxygen and room air that maintained O_2 concentration at 80%. In these chambers, the animals had sufficient space to move around and to drink and eat normally. Control animals received 1.5 ml of saline solution intraperitoneally and were exposed to room air during the experimental period. The protocol was approved by the Ethical Committee on Use and Care of Animals from the National Institute of Respiratory Diseases (Mexico).

Animal body weights were recorded every week, and visual examination of animal health was made daily. Animals exposed to 80% oxygen plus episodic administration of paraquat were killed beginning at 1, 2, 3, and 6 wk of exposure. Control animals were exposed to the paraquat vehicle and room air. Eight animals were studied at each time interval. Animals displaying low body weight together with respiratory insufficiency manifested by bradypnea, nasal twitching, and/or cyanosis were killed at the earliest designated sampling interval. Additionally, eight resistant rats were also studied. Resistant rats were defined as animals that received 6 wk of paraquat plus hyperoxia but gained weight, did not develop signs of respiratory insufficiency, and morphologically showed minimal lung lesions or no lesions at all.

After death, the left lungs were used for morphology, immunohistochemistry, and collagen determination, whereas the right lungs were used for Northern blot, real-time PCR, and lung tissue zymography. Because the model is characterized by diffuse inflammatory lesions followed by widespread fibrotic reaction involving both lungs (43, 44), we considered that lung sampling for all analyses represented the overall lesions.

Morphology. For histology and immunohistochemistry, the left lungs were instilled through a tracheal cannula at a constant pressure of 7 cmH_2O with 4% paraformaldehyde in PBS and embedded in paraffin. Sections were stained with hematoxylin-eosin and Masson's trichrome.

Detection of DNA fragmentation in situ. Cell death was explored in control and experimental lung tissues with a DNA fragmentation detection kit (Klenow-FragEL; Oncogene, Darmstadt, Germany) following the manufacturer's instructions. Briefly, deparaffinized lung sections were incubated with 100 μl of 20 μg/ml proteinase K at room temperature for 20 min. Samples were rinsed with 1× Tris-buffered saline (TBS) and incubated with 1 μg/μl of DNase I in 1× TBS/1 mM $MgSO_4$ at room temperature for 20 min. Endogenous peroxidase was inactivated with 30% H_2O_2 in methanol. Specimens were then covered with 1× Klenow equilibration buffer at room temperature for 30 min, following with 60 μl of Klenow labeling reaction mix. The slides were incubated in a humidified chamber at 37°C for 1.5 h. Samples were covered with 100 μl of blocking buffer at room temperature for 10 min, incubated with 100 μl of diaminobenzidine at room temperature for 15 min, and counterstained with 100 μl of methyl green.

Hydroxyproline measurement. Lung fragments from controls and paraquat plus oxygen-exposed rats were analyzed for hydroxyproline content as an estimate of collagen content. Lung samples were dried and hydrolyzed in 1 ml of 12 N HCl for 24 h at 110°C, and hydroxyproline colorimetric analysis was performed as described by Woessner (57). All assays were done in triplicate, and data are expressed as micrograms of hydroxyproline per milligram of lung tissue.

Immunohistochemistry. Immunoreactive TIMP-1 was identified in lung tissue sections as previously described (36, 45). Briefly, after deparaffinized tissue sections were rehydrated and blocked with 3% H_2O_2 in methanol followed by antigen retrieval in a microwave in 10 mM citrate buffer, pH 6.0, for 5 min. Tissue sections were treated with an antibody diluent with background reducing components (Dako, Carpinteria, CA) diluted 1:100 in PBS and then incubated with anti-TIMP-1 antibody (rabbit polyclonal; 200 μg/ml diluted 1:100; Santa Cruz, CA) at 4°C overnight. A secondary biotinylated anti-immunoglobulin followed by horseradish peroxidase-conjugated streptavidin (BioGenex, San Ramon, CA) was used according to the manufacturer's instructions. 3-Amino-9-ethyl-carbazole (BioGenex) in acetate buffer containing 0.05% H_2O_2 was used as substrate. The sections were counterstained with hematoxylin. The primary antibody was replaced by nonimmune serum for negative control slides.

Lung tissue gelatin zymography. Lung samples (20 mg/ml) from control and experimental animals were homogenized in 10 mM 3-[(3-cholamidopropyl)dimethylammonio]-1-propanesulfonate (Sigma), 20 mM HEPES, pH 7.5, plus 150 mM NaCl. After centrifugation, aliquots of supernatants containing 10 μg of protein were used to analyze lung tissue gelatinase activity in a gelatin substrate SDS gel as previously described (33). Serum-free conditioned medium from human lung fibroblasts and from U2-OS cells stimulated with phorbol 12-myristate 13-acetate were used as MMP-2 and MMP-9 markers, respectively. Like gels were incubated but in the presence of 20 mM EDTA. Gelatinolytic activities were quantified using 1D image analysis software (Eastman Kodak, Rochester, NY) considering the area and intensity of lysis bands. Results were expressed as relative units (net intensity $\times 10^{-4}$ per 10 μg of lung protein).

Detection of TGF-β1 by ELISA in lung extracts. Aliquots of supernatants obtained from lung homogenates were used to determine biologically active and total TGF-β1 by using an immunoassay system (Promega, Madison, WI). Activation of the latent form to detect total (active + latent) protein was performed by acid treatment following the manufacturer's instructions.

RNA isolation and Northern blot analysis. Total RNA was extracted from lung tissue using TRIzol reagent (Life Technologies, Grand Island, NY). RNA quality was assessed by

Table 1. *Genes and primers for real-time PCR*

Gene	Sense Primer (5′ to 3′)	Reverse Primer (5′ to 3′)	Product bp	Reference or Accession No.
R18S	GTAACCCGTTGAACCCCATT	CCATCCAATCGGTAGTAGCG	140	(40)
MMP-13	CATCCATCCCGAGACCTCAT	GCATGACTCTCACAATGCGA	324	M60616
MMP-2	CTATTCTGTCAGCACTTTGG	CAGACTTTGGTTCTCCAACTT	309	(56)
MMP-9	AAATGTGGGTGTACACAGGC	TCCTTGGGGCTCTCAATTTC	309	(56)
TIMP-1	GACCACCTTATACCAGCGTT	GTCACTCTCCAGTTTGCAAG	333	L29512
TIMP-2	CAACCCCATCAAGAGGATTC	CGCAAGAACCATCACTTCTC	416	U14526
TIMP-3	CAGTACATTCACACGGAAGC	TCTGTGGCATTGCTGATGCT	392	NM000362
TGF-β1	TGGAAGTGGATCCACGCGCCCAAGG	GCAGGAGCGCACGATCATGTTGGAC	242	(31)
PDGF-A	AAGCATGTGCCGGAGAAGCG	TCCTCTAACCTCACCTGGAC	305	(10)
CTGF	CCGGATCCGAGCTTTCTGGCTGCACC	GGCTGCAGTCTCCGTACATCTTCCTG	250	A gift from J. Lasky, Tulane Univ.
Angiotensin	GTTTGTTTGGACACACTGGGGT	ACAAGGGGACAGTGTGCATT	174	M121112.1

resolution on denatured 1% agarose gels and measurement of absorbance ratios at 260/280 nm. Total RNA (15 μg/lane) was fractionated on a 1% agarose gel containing 0.66 M formaldehyde (8). rRNA was visualized with ethidium bromide, and the fractionated RNA was transferred onto a Nytran transfer membrane (NEN, Boston, MA) by capillary blotting overnight. RNA was immobilized by being baked at 80°C for 2 h and then prehybridized at 42°C for 18 h in 5× SSC, 50% formamide, 5× Denhardt's solution, and 0.5% SDS containing 100 μg/ml of denatured salmon sperm DNA. Hybridization was carried out at 42°C for 18 h in hybridization buffer containing 50% dextran sulfate plus heat-denatured ^{32}P-labeled cDNA probes. Membranes were washed in 2× SSC, 0.1% SDS at 42°C, followed by 0.25× SSC, 0.1% SDS at 55°C and 0.1× SSC, 0.1% SDS at 65°C. After being dried, membranes were exposed to Kodak BIOMAX MS film at −70°C with an intensifying screen. Equal loading of RNA samples was monitored by assessing the mRNA level of glyceraldehyde-3-phosphate dehydrogenase. The cDNA probes were radiolabeled with [^{32}P]dCTP to specific activity of 200×10^6 dpm/μg using a multiprime DNA labeling kit (NEP-103; Dupont, Wilmington, DE).

RT-PCR and quantitative real-time PCR amplification. One microgram of total RNA was reverse transcribed using 2 μg of random primers and Moloney murine leukemia virus reverse transcriptase according to the manufacturer's protocol (Advantage RT-for-PCR Kit; Clontech, Palo Alto, CA).

Quantitative real-time PCR amplification was performed using i-Cycler iQ Detection System (Bio-Rad, Hercules, CA). PCR was performed with cDNA working mixture in a 25-μl reaction volume containing 3 μl of cDNA, 20 mM Tris·HCl, pH 8.3, 50 mM KCl, 2 mM $MgCl_2$, 200 μM dNTP, 1 μM specific 5′ and 3′ primers, 1.25 units of *Taq* DNA polymerase (Roche, Branchburg, NJ), and 10 nM fluorescein and dye SYBR green I 1:50,000 (Roche, Indianapolis, IN). A dynamic range was built with each product of PCR on copy number serial dilutions of 1×10^8, 1×10^6, 1×10^4, 1×10^2, and 1×10; all PCRs were performed in triplicate. Standard curves were calculated referring the threshold cycle (the PCR cycle at which a specific fluorescence becomes detectable) to the log of each cDNA dilution step (40, 47, 54). Results were expressed as the number of copies of the target gene normalized to 18S rRNA. Results are shown as percent of controls.

Some primers for PCR reactions were obtained from previously published rat sequences (10, 31, 40, 56), whereas the rest were outlined with http://bioweb.pasteur.fr/seqanal/interfaces/eprimer3.html and analyzed for specificity in Basic Local Alignment Search Tool (Table 1). All primers were obtained from GIBCO-BRL (Life Technologies). The cycling conditions for PCR amplification to MMP-2, MMP-9, MMP-13, CTGF, PDGF-A, and angiotensinogen were performed using the following protocol: initial activation of Amplitaq Gold DNA polymerase at 95°C for 7 min, 40 cycles of denaturation to 95°C/30 s, annealing to 58°C/30 s, and extension to 72°C/30 s. For amplification of TIMP-1, -2, -3, and TGF-β1, the annealing temperature was increased to 60°C. Specific amplification was confirmed by the presence of one single peak in the melting curve plots. Additionally, the PCR products were analyzed in agarose gel electrophoresis.

Statistical analysis. Values are expressed as means ± SE of the mean. Differences between experimental groups and controls were analyzed by using Dunnett's test. $P < 0.05$ was considered statistically significant.

RESULTS

General characteristics. Two clinical/morphological responses were manifested in the animal group receiving paraquat plus 80% oxygen. *1*) Animals termed "susceptible" exhibited constant loss of body weight and progressive respiratory insufficiency beginning at 1 or 2 wk of exposure; some of these susceptible rats suffered acute weight loss and severe respiratory distress. *2*) Approximately 20% of the exposed animals did not present weight loss, although they did not gain weight at the same rate as controls (Table 2) and showed no discernible respiratory symptoms throughout the 6 wk of exposure, when they were killed. These rats were named "resistant".

Histology and in situ DNA fragmentation. Morphological changes of the lung parenchyma at each sampling time are shown in Fig. 1. Control animals at all time points exhibited normal alveolar architecture (Fig. 1*A*). At 1 wk of exposure, multifocal interstitial and alveolar inflammation was observed, as was cuboidalization of the alveolar epithelium. Inflammation included polymorphonuclear and mononuclear cells (Fig. 1*B*). At 2 and 3 wk of exposure, the inflammatory process was predominantly mono-

Table 2. *Body weight at death*

	0 wk	1 wk	2 wk	3 wk	6 wk
Control	198 ± 13	207 ± 4	252 ± 16	278 ± 14	291 ± 15
Susceptible	207 ± 11	190 ± 18	185 ± 9	170 ± 10	165 ± 16
Resistant	202 ± 9	205 ± 11	223 ± 14	236 ± 17	264 ± 19

Values are means ± SE. Body weight measured in grams. Eight susceptible animals were killed at each time point. Eight resistant rats were killed at 6 wk.

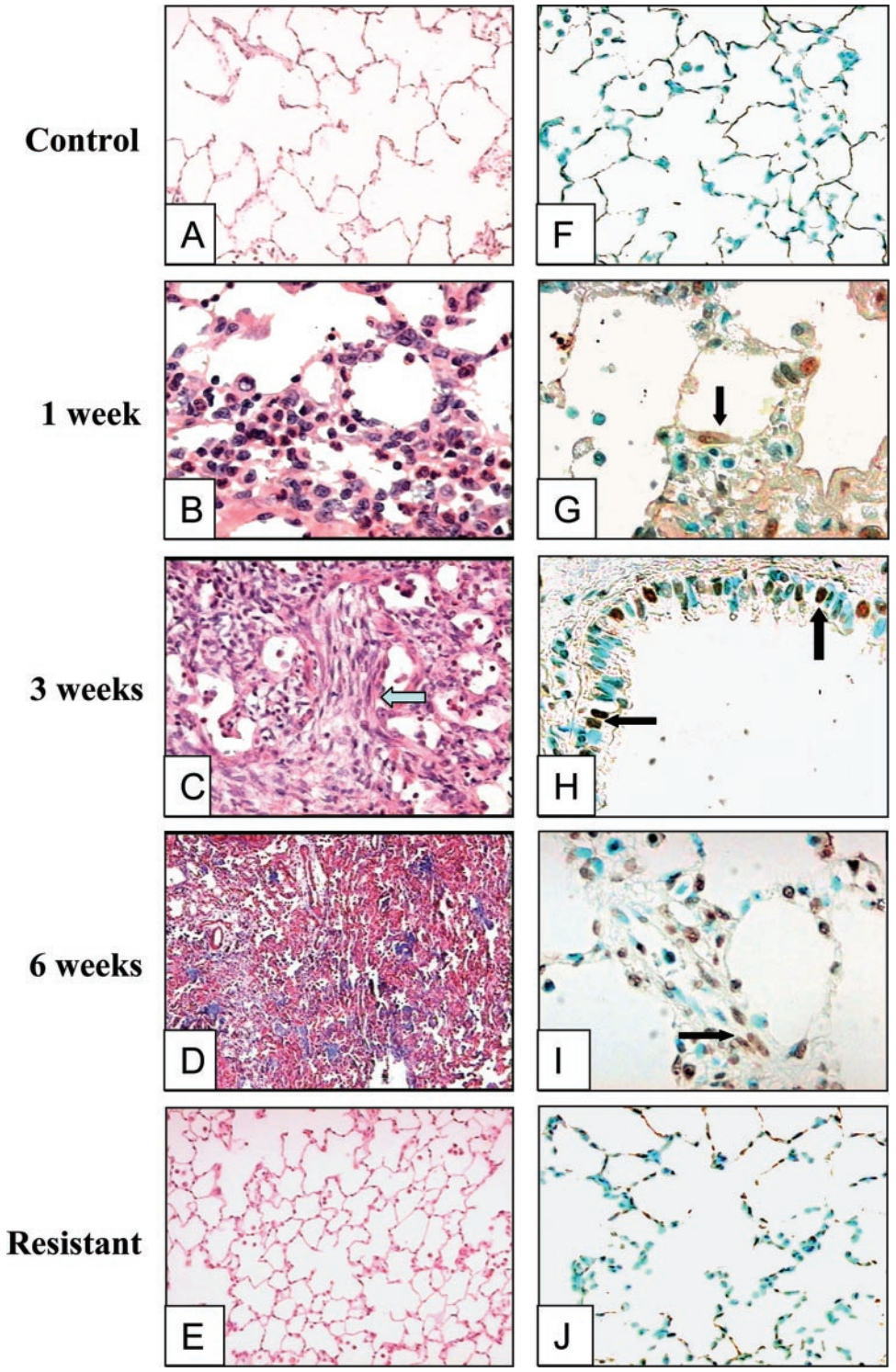

Fig. 1. Histology and in situ DNA fragmentation in control and experimental lungs. Deparaffinized lung sections from animals killed at the indicated sampling intervals were prepared for hematoxylin and eosin and Masson's trichrome staining (*left*; *A* and *C*, 20× original magnification; *B*, 40×; *D* and *E*, 10×) or for in situ DNA fragmentation (*right*; *F* and *J*, 20×; *G–I*, 40×). A fibroblastic focus is indicated by the arrow in *C*. In *G–I*, brown nuclei represent apoptotic cells (arrows), whereas green nuclei correspond to living cells.

nuclear, with interstitial and intra-alveolar lymphocytes and macrophages. Foci of densely packed interstitial fibroblasts were also found (Fig. 1*C*, arrow). At 6 wk, cell infiltrate was similar, but a more extensive collagen deposit was observed as was the severe loss of parenchymal lung architecture (Fig. 1*D*). Resistant animals exhibited normal alveolar structures with minimal or no inflammation or fibrosis, and, in general, resembled that of control animals (Fig. 1*E*).

In situ DNA fragmentation showed apoptotic cell death from the first to the sixth week (Fig. 1G). Apoptosis was diffusely distributed in the lung parenchyma and was mainly noticed in alveolar epithelial and bronchiolar cells (Fig. 1, *G* and *H*). At longer periods (6 wk), apoptotic nuclei were also observed in interstitial cells (Fig. 1*I*). Areas of intra-alveolar apoptotic inflammatory cells were also seen throughout the experiment. Resistant rats behaved as con-

trols (Fig. 1*F*), and few, if any, apoptotic cells were found (Fig. 1*J*).

Lung collagen expression and content. Paraquat plus oxygen-exposed rats showed a progressive increase of lung collagen when compared with control animals, paralleling morphological results. As illustrated in Fig. 2*A*, lung collagen quantified by hydroxyproline was ~50% increased over control levels at the third and sixth weeks ($P < 0.05$). Resistant rats showed normal values. Similarly, paraquat plus hyperoxia exposure resulted in a marked upregulation of pro-α_1(I) collagen transcript levels that was also observed at the third and sixth weeks (Fig. 2*B*).

Real-time PCR. An example of a real-time PCR experiment is shown in Fig. 3*A*. The reaction was linear over nine orders of magnitude of starting cDNA standards, with a detection sensitivity of 10 molecules and efficiency of 95.3% (Fig. 3*A*). Correlation coefficients of such standard curves were consistently >0.99. Figure 3*B* illustrates the melt-curve plot of the amplified PCR cDNAs shown in Fig. 3*A*, demonstrating the amplification of one specific product.

Levels of MMP-2, MMP-8, MMP-9, MMP-13, TIMP-1, TIMP-2, TIMP-3, TGF-β1, PDGF-A, CTGF, and angiotensinogen gene expression were assessed by quantitative real-time PCR in aliquots from whole lung homogenates of experimental and control rats. The effect of paraquat plus hyperoxia treatment was selective and showed temporal differences. Regarding MMPs (Fig. 4), the most marked effect was a significant reduction in the mRNA expression of both collagenases MMP-8 and MMP-13 from the first to the sixth week compared with controls (Fig. 4, *A* and *B*). Resistant rats showed no significant changes compared with control animals. No significant difference in lung gelatinases A and B (MMP-2 and MMP-9) mRNA expression was found between controls and experimental samples (not shown).

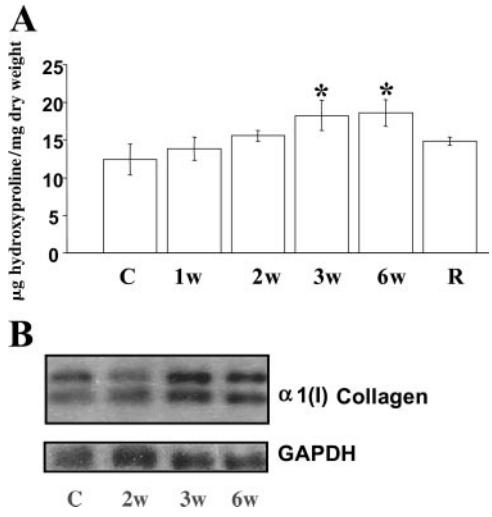

Fig. 2. Lung collagen quantification. *A*: relative content of hydroxyproline per dry weight. A significant increase of hydroxyproline can be observed after the 3rd wk (w) of exposure to paraquat and hyperoxia. The resistant (R) animals behave as unexposed animals. *$P < 0.05$. *B*: Northern blot analysis showing upregulation of α_1(I) collagen expression at 3 and 6 wk. GAPDH, glyceraldehyde-3-phosphate dehydrogenase. C, controls.

As illustrated in Fig. 5, TIMP-1 exhibited a significant increase from the second week until the final period of the experiment. Resistant rats did not show differences with controls. By contrast, TIMP-2 and TIMP-3 showed no changes at any time (not shown).

TGF-β1 gene expression showed a significant increase from the first- until the third-week interval of paraquat plus oxygen exposure (Fig. 6*A*). Likewise, analysis of lung homogenates revealed a significant increase of total (active and latent) TGF-β1 protein levels at 2 and 3 wk ($P < 0.01$ and 0.05, respectively; Fig. 6*B*). The majority of this protein was in the latent (inactive) form, measurable in the bioassay only after acid activation. The amount of spontaneously active TGF-β1 was low (5–10 ng/ml) and was found elevated in the experimental animals at 2 wk of paraquat plus oxygen exposure ($P < 0.05$; Fig. 6*C*). Levels of resistant rats were similar to controls. PDGF-A, CTGF, and angiotensinogen mRNA levels showed no differences with control lungs (not shown).

Lung localization of TIMP-1 by immunohistochemistry. Immunoreactive TIMP-1 was not detected in normal lungs (Fig. 7*A*). By contrast, lungs from rats injured with paraquat plus hyperoxia showed, from the first week on, increased TIMP-1 expression mainly localized in alveolar macrophages and occasionally in bronchiolar and alveolar epithelial cells and in smooth muscle cells from vessels (Fig. 7, *B–D*). No differences in TIMP-1 cell localization were observed with the progression of the lung lesions, but the inhibitor was primarily noticed in injured areas. Negative controls incubated with nonimmune serum were negative (Fig. 7*E*).

Lung tissue zymography. Aliquots of lung tissue extract supernatants from control and experimental animals containing ~10 μg of protein were used. A representative zymogram showing two samples from each time period is represented in Fig. 8. Compared with control rats, experimental animals receiving the double aggression showed from the first week on an increase in pro-MMP-2 and its active form represented by the lower molecular band of ~62 kDa. A two- to threefold increase was revealed by densitometric quantification of the surface and intensity of lysis bands of zymograms derived from five different animals in each group (Fig. 8). Resistant animals behaved similarly to control. Likewise, an increase in the band corresponding to MMP-9 was noticed mainly at 3 and 6 wk in most injured animals (Fig. 8). At these periods, densitometric quantification showed a twofold increase compared with controls. A mild increase was observed in some resistant animals, but no significant difference was observed when compared with controls.

DISCUSSION

As discussed earlier (43, 44), an acceptable experimental model of diffuse interstitial pulmonary fibrosis should *1*) be progressive and potentially lethal; *2*) de-

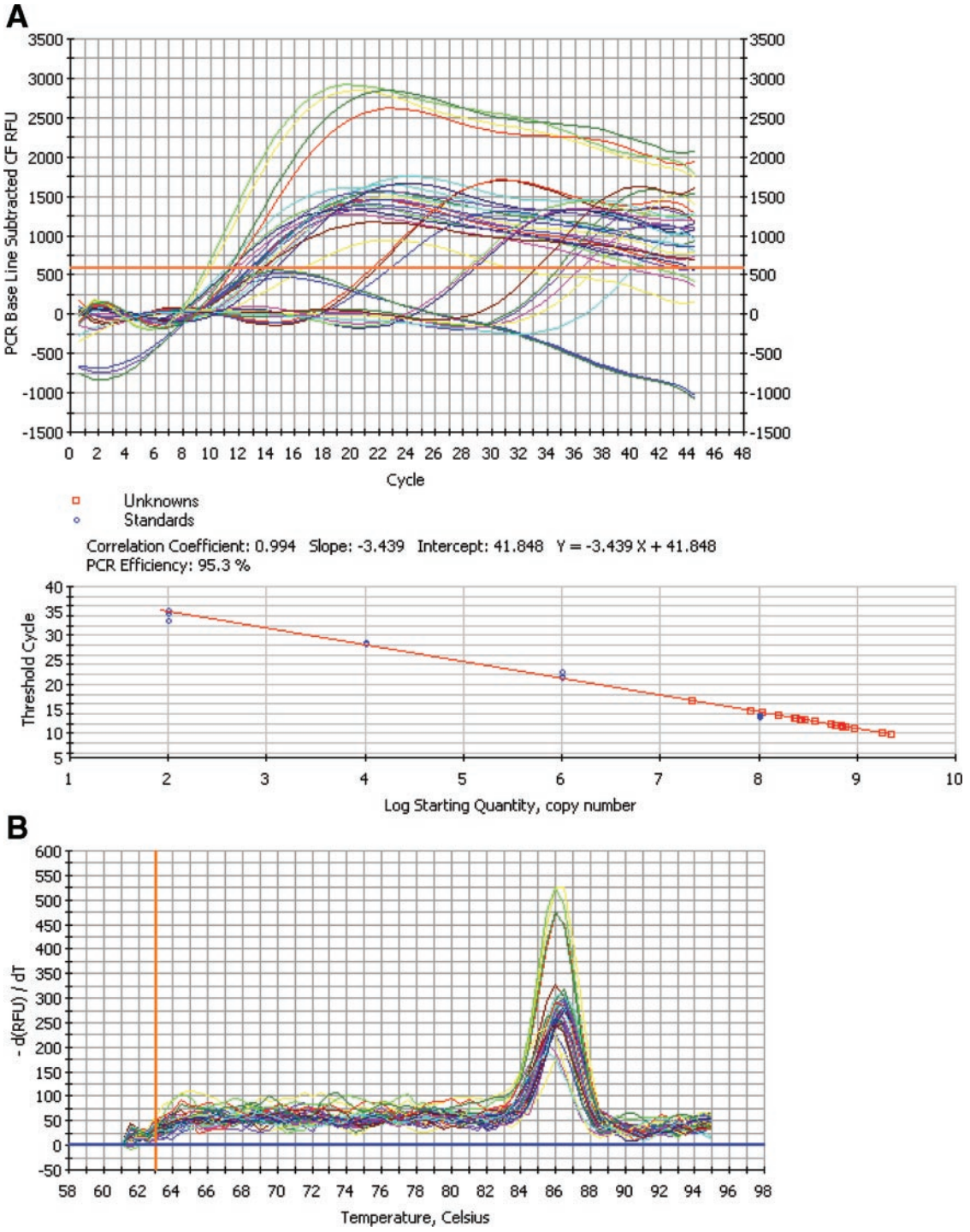

Fig. 3. *A*, *top*: amplification of R18S detected by changes in fluorescence (CF RFU) in a real-time PCR setting. Thirty-six samples in triplicate were assayed against 5 DNA standards spanning 8 logs. *A*, *bottom*: standard curve of threshold cycle against known quantities of DNA standards. *B*: melt-curve plots representing products from the amplification shown in *A*.

velop clinical and functional data of pulmonary insufficiency; and *3*) resemble the histological features of the human disease. Previous morphological and biochemical characterization of the model used here demonstrated that each of these criterion is fulfilled (44).

An important additional observation in the present study was the finding of resistant animals. Thus histology and collagen accumulation data suggest that although most animals appeared to be susceptible to the combination of paraquat plus hyperoxia, others survived 6 wk with only minor or no lesions at all. These resistant rats displayed weight gain and complete lack of respiratory insufficiency throughout the exposure period. Although it is theoretically feasible

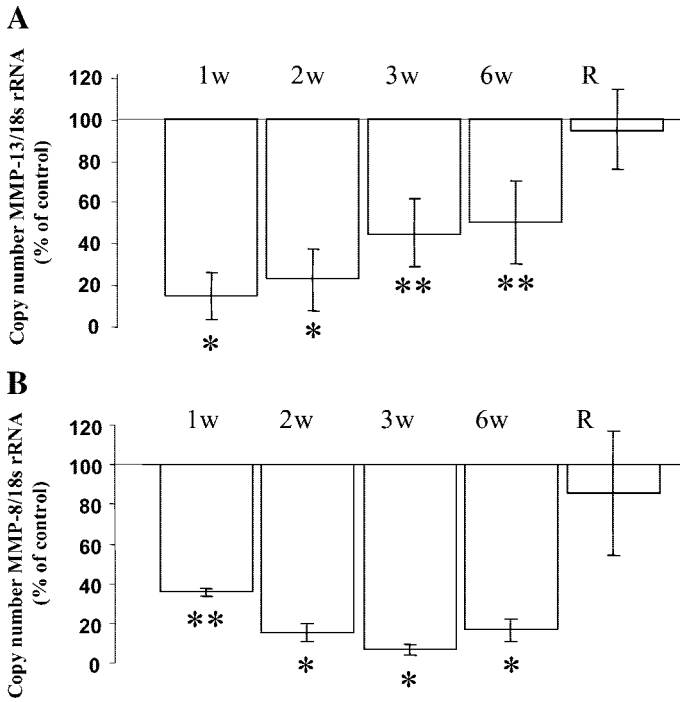

Fig. 4. Quantitative real-time PCR. Gene expression of matrix metalloproteinases (MMP)-13 (*A*) and MMP-8 (*B*) normalized for R18S rRNA in 6–8 control and experimental lung cDNA samples. Results are expressed as percent of controls. $^{*}P < 0.01$; $^{**}P < 0.05$.

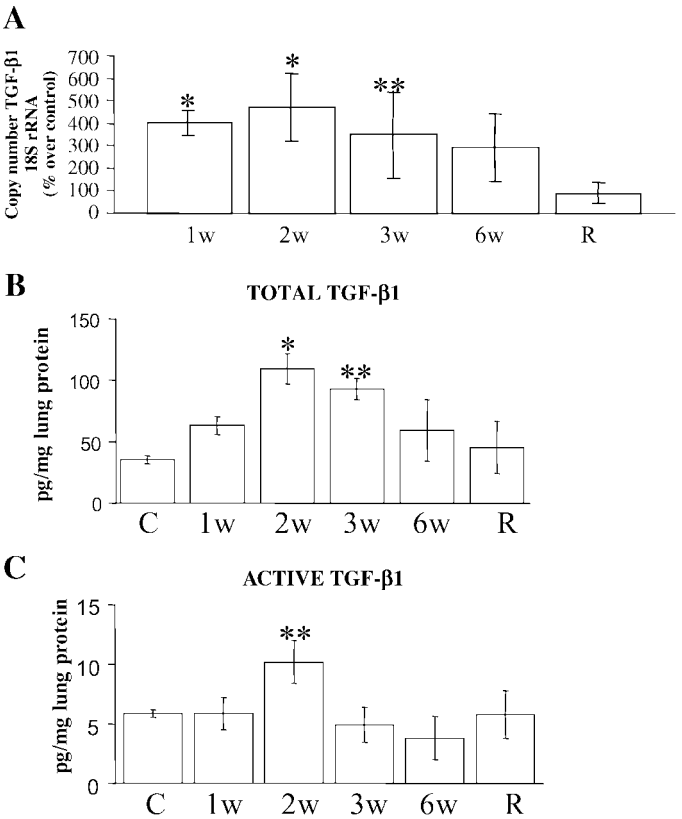

Fig. 6. *A*: real-time PCR for transforming growth factor (TGF)-β1. An increased gene expression is observed in the first 3 wk. $^{*}P < 0.01$; $^{**}P < 0.05$. *B* and *C*: levels of active and total (active + latent) TGF-β1 in lung homogenates. $^{*}P < 0.01$; $^{**}P < 0.05$. C, control.

that some animals surviving 6 wk had developed at earlier time points more severe lesions from which they recovered before death, a sequential analysis of body weights at earlier time points does not support such an interpretation.

Lung fibrosis may be regarded as pathological wound repair after injury with excessive fibroproliferation and accumulation of extracellular matrix. Nevertheless, the molecular mechanisms involved in the extensive structural remodeling that characterizes the fibrotic response are not completely understood. However, a growing body of evidence strongly suggests that abnormal expression/activity of MMPs and TIMPs plays a role in this process (13, 33–36, 45). In this work, a noteworthy decreased expression of the two major collagenases present in adult rat, equivalent orthologs of human neutrophil collagenase (MMP-8) (5) and collagenase-3 (MMP-13) (12), was observed. These enzymes share the unique ability to cleave the native helix of fibrillar collagens, which are the most abundant proteins in fibrotic tissues. In addition, we found that TIMP-1 expression was increased in parallel to fibrosis development. These findings support the notion that an imbalance between the process of matrix degradation and their inhibition actively participates in the development of lung fibrogenesis and that progression of fibrosis is associated with inhibition of matrix breakdown. Interestingly, resistant animals showed no changes in collagenases or TIMP-1 expression compared with control rats.

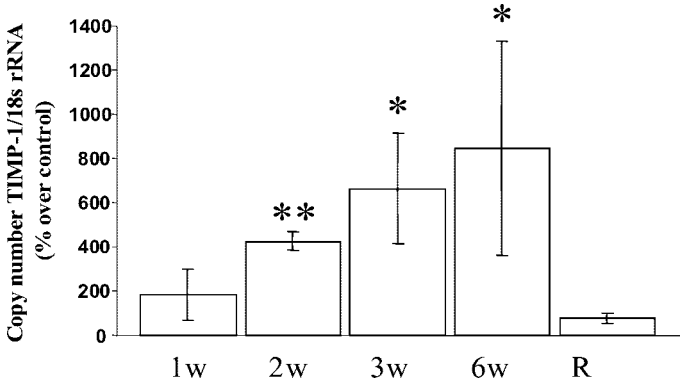

Fig. 5. Comparison of tissue inhibitors of metalloproteinases (TIMP)-1 mRNA levels relative to 18S rRNA in control and experimental rats using real-time PCR. A significant increase of the target gene is observed from the 2nd wk. $^{**}P < 0.05$; $^{*}P < 0.01$.

Studies regarding the putative role of MMP-8 or neutrophil collagenase in pulmonary fibrosis are lacking. MMP-8 preferentially degrades type I collagen, and it has been recently suggested that this enzyme, when cloned in an adenoviral vector and delivered to cirrhotic rat livers, is able to markedly reverse the fibrotic lesion (14). Likewise, although high levels of MMP-8 have been found in bronchoalveolar lavage from patients with idiopathic pulmonary fibrosis, the presence of this enzyme in situ is practically nonexistent (21, 45).

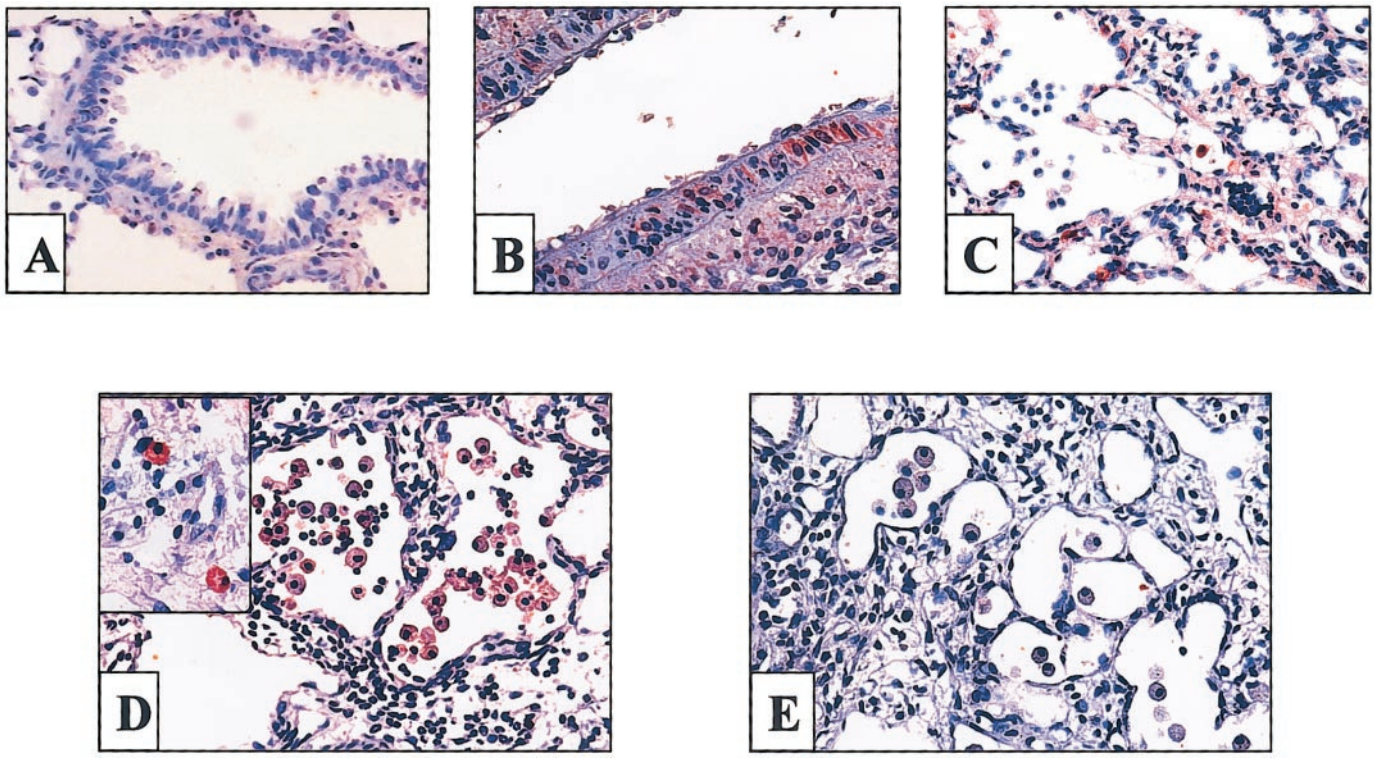

Fig. 7. TIMP-1 immunolocalization in experimental and control lungs. *A*: no signal is observed in normal lung. *B*: TIMP-1 immunoreactive bronchiolar epithelial cells after 2-wk exposure to paraquat and hyperoxia. *C*: immunoreactive signal in some inflammatory and alveolar epithelial cells. *D*: positive free alveolar macrophages. *Inset*: 2 intensely stained interstitial macrophages. *E*: negative control omitting the primary antibody.

On the other hand, remodeling of fibrillar collagen in mouse and rat tissues has been widely attributed to the activity of MMP-13, the main collagenase identified in this species. In humans, MMP-13 was originally identified in breast carcinoma (12) and is characterized by a potent degrading activity against a wide spectrum of extracellular matrix proteins besides fibrillar collagen. MMP-13 has been suggested to play a major role in the pathogenesis of tissue destruction in rheumatoid arthritis (37). However, its expression has not been revealed in human normal or fibrotic lung tissue (45).

MMP-13 gene expression has been previously evaluated in bleomycin-induced fibrosis in mice, but in contrast to our findings, no changes were found (48). In the present study, we also looked for murine collagenase-like A, the putative ortholog of human MMP-1 in murines (6), but gene expression was found only in embryonic rat and not in adult normal or experimental lungs (not shown).

TIMP-1 gene expression was consistently upregulated in the injured rats evolving to fibrosis. The inhibitor was primarily expressed on alveolar macrophages but also in alveolar epithelial cells, and it was spatially restricted to areas of lung injury. In this context, it is important to emphasize that TIMP-1 seems to play a major role in lung fibrosis in rodents. This inhibitor has been shown to be markedly upregulated during experimental lung fibrosis, and it even seems to be selectively and markedly increased in a murine model of bleomycin-induced pulmonary fibrosis (25, 48). Furthermore, high levels of TIMP-1 are present early after bleomycin exposure and persist for weeks after the initial insult (25). Moreover, it has been recently demonstrated that a crucial difference between a fibrosis-prone and a fibrosis-resistant mouse strain after transient lung overexpression of active TGF-β1 is associated with the regulation of TIMP-1 (22). Thus the susceptible C57BL/6 showed a strong upregulation of TIMP-1 gene in their lungs in vivo and in their fibroblasts in vitro in contrast to a weak induction in the resistant BALB/c, suggesting that the differences in extent of lung fibrosis might be in part due to altered extracellular matrix turnover provoked by TIMP-1 expression.

In our study, the increased expression of TIMP-1 preceded increased accumulation of collagen, suggesting that fibrillar matrix proteins are laid down into a microenvironment in which matrix degradation is already reduced.

The mechanisms underlying the increase of TIMP-1 may be at least partially related to an upregulation of TGF-β, a prototype of a profibrotic factor found elevated at the gene and protein level during the first 3 wk. It is well known that the fibrogenic effect of TGF-β is not only caused by stimulation of matrix synthesis but also by a complex regulation of MMP and TIMP interaction, including stimulation of TIMP-1 expression (19, 27, 38). It is important to emphasize that although TGF-β provokes a decrease of expression of MMP-1 and MMP-8, it seems to be a potent inducer of

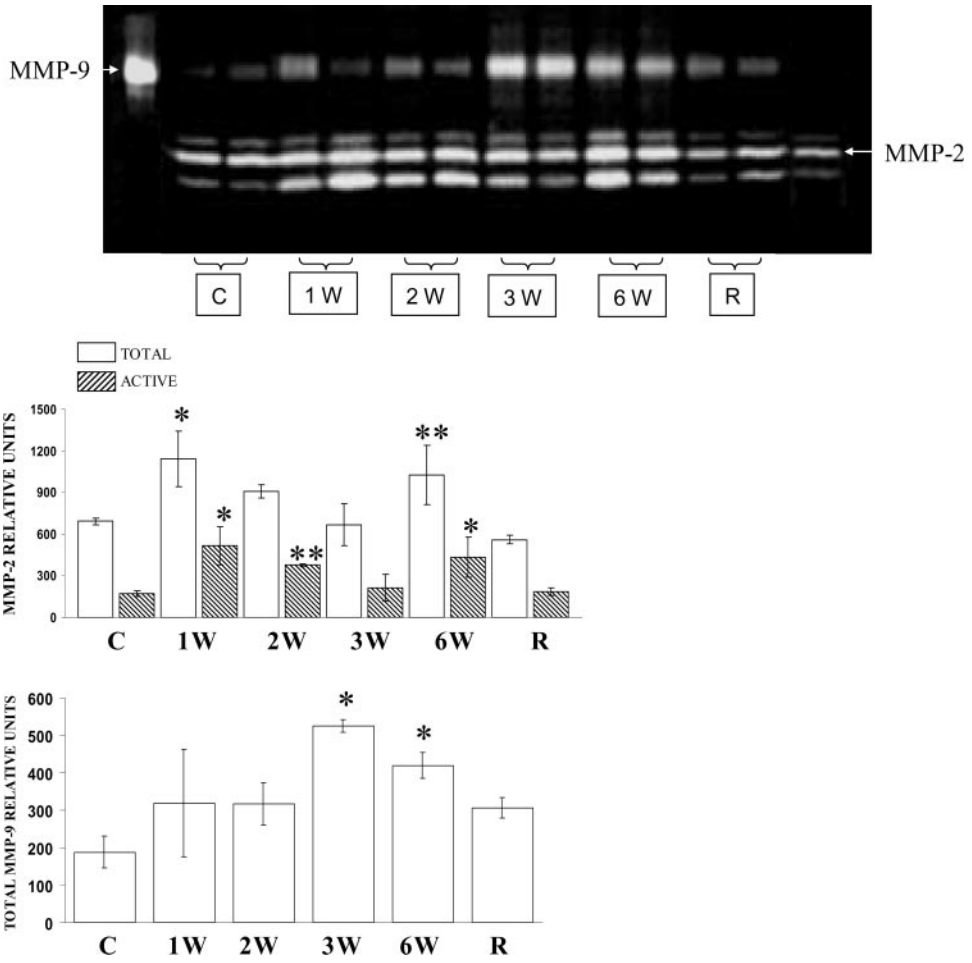

Fig. 8. Lung tissue zymography. Samples containing ~10 μg of protein were mixed with an equal volume of sample buffer containing 3% SDS. Zones of enzymatic activity appear as clear bands over a dark background. Gelatinolytic activity bands were inhibited by EDTA. Serum-free conditioned medium from human lung fibroblasts was used as MMP-2 marker (*middle*) and from phorbol 12-myristate 13-acetate-stimulated U2-OS cells as marker of MMP-9 (*bottom*). $*P < 0.01$; $**P < 0.05$. paraquat + hyperoxia-susceptible-exposed animals after 1, 2, 3, and 6 wk (1W, 2W, 3W, 6W).

MMP-13 gene expression, at least in vitro (32, 53). However, in vivo studies using transgenic mice overexpressing TGF-β have suggested a downregulatory effect (41).

MMP-2 did not display changes in gene expression; however, an important increase mainly in the lung active form was observed from the beginning of the double aggression. This finding would suggest an upregulation of membrane type 1 MMP (30, 58). Results regarding MMP-9 were to some extent paradoxical. Thus whereas no changes were observed at the gene expression level, an increase of MMP-9 protein was noticed in zymograms. This finding may be attributed, at least partially, to the leukocyte infiltrate since these cells carry the preformed enzyme in specific granules (30, 58). MMP-2 and MMP-9 activities have broad substrate specificity, which includes type IV collagen, the main component of basement membrane, and increased activities of these enzymes may contribute to its disruption. In this context, it has been suggested that epithelial basement membrane integrity plays an important role in determining normal lung reepithelialization or a fibrotic response (34). In bleomycin-induced lung fibrosis, a coincidental increase of MMP-9 activity and disruption of the alveolar epithelial basement membrane have been found (59). Interestingly, both MMPs have been found elevated in human pulmonary fibrosis (13, 44). Additionally, it is important to emphasize that gelatinases have other non-matrix substrates that can enhance a fibrotic reaction. Thus, for example, cell surface-localized MMP-9 is able to proteolytically cleave latent TGF-β, providing a potentially important mechanism for TGF-β activation and tissue remodeling (60).

Alveolar epithelial loss, putatively caused by apoptosis, is a common finding in pulmonary fibrosis, and several mechanisms seem to be involved (11, 17, 18, 52). Lung fibroblasts obtained from patients with idiopathic pulmonary fibrosis induce alveolar epithelial cell apoptosis by secreting angiotensin peptides (55), whereas Fas-signaling pathway has been found upregulated in epithelial cells from both human and experimental fibrotic lungs (11, 18, 26). Actually, it has been demonstrated that a single instillation of bleomycin leads to the appearance of apoptosis in bronchial and alveolar epithelial cells that in turn is accompanied with a progression of fibrosis (18). In our study, increased apoptotic epithelial cell death was observed from the first week and continues for >6 wk of paraquat plus hyperoxia exposure, suggesting that may also play a role in the development of fibrosis, altering epithelium self-renewing. Importantly, although epi-

thelial cells within lesions undergo heavy labeling of fragmented DNA, this process was less intense in normal regions of the parenchyma, which is consistent with a pivotal role for apoptosis in determining the rate of epithelial repair (50). Interestingly, resistant rats mostly behave like control noninjured animals.

DNA fragmentation labeling of interstitial and alveolar inflammatory cells within lesions at all periods of the experiment was suggestive of clearance of these cells by apoptosis. Likewise, some interstitial apoptosis could also correspond to fibroblasts as part of the lung remodeling process.

In summary, we found a strong correlation between decreased gene expression of interstitial collagenases and increased gene expression of TIMP-1 and TGF-β with morphological and biochemical evidence of extracellular matrix accumulation, suggesting that dysregulated matrix remodeling is likely to contribute to the pathology of paraquat plus hyperoxia-induced pulmonary fibrosis. Increases in gelatinolytic activity and epithelial apoptosis were also important features of this model that preceded the fibrotic response. The basis for differences in susceptibility among animals is at present unknown but will be an interesting topic for future inquiry.

REFERENCES

1. **Adamson IYR, Young L, and Bowden DH.** Relationship of alveolar epithelial injury and repair to the induction of pulmonary fibrosis. *Am J Pathol* 130: 377–383, 1988.
2. **Antoniades NH, Bravo M, Avila R, Galanopoulus T, Neville J, and Selman M.** Platelet-derived growth factor in idiopathic pulmonary fibrosis. *J Clin Invest* 86: 1055–1064, 1990.
3. **Baker AH, Zaltsman AB, George SJ, and Newby AC.** Divergent effects of tissue inhibitor of metalloproteinase-1, -2, or -3 overexpression on rat vascular smooth muscle cell invasion, proliferation, and death in vitro. TIMP-3 promotes apoptosis. *J Clin Invest* 101: 1478–1487, 1998.
4. **Baker HJ, Lindsey JR, and Weisbroth SH.** The laboratory rat. In: *Biology and Diseases*, edited by American College of Laboratory, New York: Academic, 1979 (Animal Medicine Series).
5. **Balbin M, Fueyo A, Knauper V, Lopez JM, Alvarez J, Sanchez LM, Quesada V, Bordallo J, Murphy G, and Lopez-Otin C.** Collagenase 2 (MMP-8) expression in murine tissue-remodeling processes. Analysis of its potential role in postpartum involution of the uterus. *J Biol Chem* 273: 23959–23968, 1998.
6. **Balbin M, Fueyo A, Knauper V, Lopez JM, Alvarez J, Sanchez LM, Quesada V, Bordallo J, Murphy G, and Lopez-Otin C.** Identification and enzymatic characterization of two diverging murine counterparts of human interstitial collagenase (MMP-1) expressed at sites of embryo implantation. *J Biol Chem* 276: 10253–10262, 2001.
7. **Barrios R, Pardo A, Ramos C, Montaño M, Ramírez R, and Selman M.** Upregulation of acidic fibroblast growth factor during development of experimental lung fibrosis. *Am J Physiol Lung Cell Mol Physiol* 273: L451–L458, 1997.
8. **Becerril C, Pardo A, Montaño M, Ramos C, Ramírez R, and Selman M.** Acidic fibroblast growth factor (FGF-1) induces an antifibrogenic phenotype in human lung fibroblasts. *Am J Respir Cell Mol Biol* 20: 1020–1027, 1999.
9. **Castoldi G, Di Gioia CR, Pieruzzi F, D'Orlando C, Van De Greef W, Busca G, Sperti G, and Stella A.** ANG II increases TIMP-1 expression in rat aortic smooth muscle cells in vivo. *Am J Physiol Heart Circ Physiol* 284: H635–H643, 2003.
10. **Dobrian A, Wade S, and Prewitt R.** PDGF-A expression correlates with blood pressure and remodeling in 1K1C hypertensive rat arteries. *Am J Physiol Heart Circ Physiol* 276: H2159–H2167, 1999.
11. **Fine A, Anderson N, Rothstein T, Williams M, and Gochuico B.** FAS expression in pulmonary alveolar type II cells. *Am J Physiol Lung Cell Mol Physiol* 273: L64–L71, 1997.
12. **Freije JM, Diez-Itza I, Balbin M, Sanchez LM, Blasco R, Tolivia J, and Lopez-Otin C.** Molecular cloning and expression of collagenase-3, a novel human matrix metalloproteinase produced by breast carcinomas. *J Biol Chem* 269: 16766–16773, 1994.
13. **Fukuda Y, Ishizaki M, Kudoh S, Kitaichi M, and Yamanaka N.** Localization of matrix metalloproteinases-1, -2, and -9 and tissue inhibitor of metalloproteinase-2 in interstitial lung diseases. *Lab Invest* 78: 687–698, 1998.
14. **Garcia-Banuelos J, Siller-Lopez F, Miranda A, Aguilar LK, Aguilar-Cordova E, and Armendariz-Borunda J.** Cirrhotic rat livers with extensive fibrosis can be safely transduced with clinical-grade adenoviral vectors. Evidence of cirrhosis reversion. *Gene Ther* 9: 127–134, 2002.
15. **Gómez D, Alonso D, Yoshiji U, and Thorgeirsson P.** Tissue inhibitors of metalloproteinases: structure, regulation and biological functions. *Eur J Cell Biol* 74: 111–122, 1997.
16. **Guedez L, Stetler-Stevenson WG, Wolff L, Wang L, Fukushima P, Mansoor A, and Stetler-Stevenson M.** In vitro suppression of programmed cell death of B cells by tissue inhibitor of metalloproteinases-1. *J Clin Invest* 102: 2002–2010, 1998.
17. **Hagimoto N, Kuwano K, Miyazaki H, Kunitake R, Fujita M, Kawasaki M, Kanika Y, and Hara N.** Induction of apoptosis and pulmonary fibrosis in mice in response to ligation of FAS antigen. *Am J Respir Cell Mol Biol* 17: 272–278, 1997.
18. **Hagimoto N, Kuwano K, Nomoto Y, Kunitake R, and Hara N.** Apoptosis and expression of FAS/FAS ligand mRNA in bleomycin induced pulmonary fibrosis in mice. *Am J Respir Cell Mol Biol* 16: 91–101, 1997.
19. **Hall MC, Young DA, Waters JG, Rowan AD, Chantry A, Edwards DR, and Clark IM.** The comparative role of activator protein 1 and Smad factors in the regulation of TIMP-1 and MMP-1. Gene expression by transforming growth factor-β1. *J Biol Chem* 278: 10304–10313, 2003.
20. **Haschek WM, Reiser KM, Klein-Szanto AJP, Last JA, and Witschi HP.** Potentiation of butylated hydroxytoluene induced lung damage by oxygen: cell kinetics and collagen metabolism. *Am Rev Respir Dis* 127: 28–34, 1983.
21. **Henry MT, McMahon K, Mackarel AJ, Prikk K, Sorsa T, Maisi P, Sepper R, Fitzgerald MX, and O'Connor CM.** Matrix metalloproteinases and tissue inhibitor of metalloproteinase-1 in sarcoidosis and IPF. *Eur Respir J* 20: 1220–1227, 2002.
22. **Kolb M, Bonniaud P, Galt T, Sime PJ, Kelly MM, Margetts PJ, and Gauldie J.** Differences in the fibrogenic response after transfer of active transforming growth factor-β1 gene to lungs of "fibrosis-prone" and "fibrosis-resistant" mouse strains. *Am J Respir Cell Mol Biol* 27: 141–150, 2002.
23. **Leivonen SK, Chantry A, Hakkinen L, Han J, and Kahari VM.** Smad3 mediates transforming growth factor-β-induced collagenase-3 (matrix metalloproteinase-13) expression in human gingival fibroblasts. Evidence for cross-talk between Smad3 and p38 signaling pathways. *J Biol Chem* 277: 46338–46346, 2002.
24. **Liu JY, Morris GF, Lei WH, Hart CE, Lasky JA, and Brody AR.** Rapid activation of PDGF-A and -B expression at sites of lung injury in asbestos-exposed rats. *Am J Respir Cell Mol Biol* 17: 129–140, 1997.
25. **Madtes DK, Elston AL, Kaback LA, and Clark JG.** Selective induction of tissue inhibitor of metalloproteinase-1 in bleomycin-induced pulmonary fibrosis. *Am J Respir Cell Mol Biol* 24: 599–607, 2001.
26. **Maeyama T, Kuwano K, Kawasaki M, Kunitake R, Hagimoto N, Matsuba T, Yoshimi M, Inoshima I, Yoshida K, and Hara N.** Upregulation of Fas-signalling molecules in lung epithelial cells from patients with idiopathic pulmonary fibrosis. *Eur Respir J* 17: 180–189, 2001.
27. **McAnulty RJ, Campa JS, Cambrey AD, and Laurent GJ.** The effect of transforming growth factor β on rates of procollagen

synthesis and degradation in vitro. *Biochim Biophys Acta* 1091: 231–235, 1991.
28. **McCawley LJ and Matrisian LM.** Matrix metalloproteinases: they're not just for matrix anymore. *Curr Opin Cell Biol* 13: 534–540, 2001.
29. **Murphy FR, Issa R, Zhou X, Ratnarajah S, Nagase H, Arthur MJ, Benyon C, and Iredale JP.** Inhibition of apoptosis of activated hepatic stellate cells by tissue inhibitor of metalloproteinase-1 is mediated via effects on matrix metalloproteinase inhibition: implications for reversibility of liver fibrosis. *J Biol Chem* 277: 11069–11076, 2002.
30. **Nagase H and Woessner JF.** Matrix metalloproteinases. *J Biol Chem* 274: 21491–21494, 1999.
31. **Napoli J, Prentice D, Niinami C, Bishop GA, Desmond P, and McCaugham GW.** Sequential increases in the intrahepatic expression of epidermal growth factor, basic fibroblast growth factor, and transforming growth factor β in a bile duct ligated rat model of cirrhosis. *Hepatology* 26: 624–633, 1997.
32. **Palosaari H, Wahlgren J, Larmas M, Ronka H, Sorsa T, Salo T, and Tjaderhane L.** The expression of MMP-8 in human odontoblasts and dental pulp cells is downregulated by TGF-β1. *J Dent Res* 79: 77–84, 2000.
33. **Pardo A, Barrios R, Maldonado V, Meléndez J, Ruiz V, Segura L, Sznajder JI, and Selman M.** Gelatinases A and B are upregulated in lung rats by subacute hyperoxia. Pathogenetic implications. *Am J Pathol* 153: 833–844, 1998.
34. **Pardo A and Selman M.** Molecular mechanisms of pulmonary fibrosis. *Front Biosci* 7: d1743–d1761, 2002.
35. **Pardo A, Selman M, Ridge K, Barrios R, and Sznajder JI.** Increased expression of gelatinases and collagenase in rat lungs exposed to 100% oxygen. *Am J Respir Crit Care Med* 154: 1067–1075, 1996.
36. **Pérez-Ramos J, Segura L, Ramírez R, Vanda B, Selman M, and Pardo A.** Matrix metalloproteinases 2, 9, and 13 and tissue inhibitor of metalloproteinases 1 and 2 in early and late lesions of experimental lung silicosis. *Am J Respir Crit Care Med* 160: 1274–1282, 1999.
37. **Petrow PK, Wernicke D, Schulze Westhoff C, Hummel KM, Brauer R, Kriegsmann J, Gromnica-Ihle E, Gay RE, and Gay S.** Characterization of the cell type-specificity of collagenase 3 mRNA expression compared with membrane type 1 matrix metalloproteinase and gelatinase A in the synovial membrane in rheumatoid arthritis. *Ann Rheum Dis* 61: 391–397, 2002.
38. **Raghow R, Postlethwaite AE, Keski-Oja J, Moses HL, and Kang AH.** Transforming growth factor-β increases steady state levels of type I procollagen and fibronectin messenger RNAs posttranscriptionally in cultured human dermal fibroblasts. *J Clin Invest* 79: 1285–1288, 1987.
39. **Raghu G, Striker LJ, Hudson LD, and Striker GE.** Extracellular matrix in normal and fibrotic human lungs. *Am Rev Respir Dis* 131: 281–289, 1985.
40. **Schmittgen TD and Zakrajsek BA.** Effect of experimental treatment on housekeeping gene expression: validation by real-time, quantitative RT-PCR. *J Biochem Biophys Methods* 46: 69–81, 2000.
41. **Seeland U, Haeuseler C, Hinrichs R, Rosenkranz S, Pfitzner T, Scharffetter-Kochanek K, and Bohm M.** Myocardial fibrosis in transforming growth factor-β1 transgenic mice is associated with inhibition of interstitial collagenase. *Eur J Clin Invest* 32: 295–303, 2002.
42. **Selman M, King TE, and Pardo A.** Idiopathic pulmonary fibrosis: prevailing and evolving hypotheses about its pathogenesis and implications for therapy. *Ann Intern Med* 134: 136–151, 2001.
43. **Selman M, Montano M, Montfort I, and Perez-Tamayo R.** A new model of diffuse interstitial pulmonary fibrosis in the rat. *Exp Mol Pathol* 43: 375–387, 1985.
44. **Selman M, Montano M, Ramos C, Barrios R, and Perez-Tamayo R.** Experimental pulmonary fibrosis induced by paraquat plus oxygen in rats: a morphologic and biochemical sequential study. *Exp Mol Pathol* 50: 147–166, 1989.
45. **Selman M, Ruiz V, Cabrera S, Segura L, Ramírez R, Barrios R, and Pardo A.** TIMP -1, -2, -3, and -4 in idiopathic pulmonary fibrosis. A prevailing nondegradative lung microenvironment? *Am J Physiol Lung Cell Mol Physiol* 279: L562–L574, 2000.
46. **Shihab FS, Bennett WM, Tanner AM, and Andoh TF.** Angiotensin II blockade decreases TGF-β1 and matrix proteins in cyclosporine nephropathy. *Kidney Int* 52: 660–673, 1997.
47. **Simpson DA, Feeney S, Boyle C, and Stitt AW.** Retinal VEGF mRNA measured by SYBR green I fluorescence: a versatile approach to quantitative PCR. *Mol Vis* 6: 178–183, 2000.
48. **Swiderski RE, Dencoff JE, Floerchinger CS, Shapiro SD, and Hunninghake GW.** Differential expression of extracellular matrix remodeling genes in a murine model of bleomycin-induced pulmonary fibrosis. *Am J Pathol* 152: 821–828, 1998.
49. **Tabibzadeh S.** Homeostasis of extracellular matrix by TGF-β and lefty. *Front Biosci* 7: d1231–d1246, 2002.
50. **Uhal BD.** Cell cycle kinetics in the alveolar epithelium. *Am J Physiol Lung Cell Mol Physiol* 272: L1031–L1045, 1997.
51. **Uhal BD, Joshi I, Hughes W, Ramos C, Pardo A, and Selman M.** Alveolar epithelial cell death adjacent to underlying myofibroblasts in advanced fibrotic human lung. *Am J Physiol Lung Cell Mol Physiol* 275: L1192–L1199, 1998.
52. **Uhal BD, Joshi I, True A, Mundle S, Raza A, Pardo A, and Selman M.** Fibroblasts isolated after fibrotic lung injury induce apoptosis of alveolar epithelial cells in vitro. *Am J Physiol Lung Cell Mol Physiol* 269: L819–L828, 1995.
53. **Uria JA, Jimenez MG, Balbin M, Freije JM, and Lopez-Otin C.** Differential effects of transforming growth factor-β on the expression of collagenase-1 and collagenase-3 in human fibroblasts. *J Biol Chem* 273: 9769–9777, 1998.
54. **Von Schnakenburg C, Strehlau J, Ehrich JH, and Melk A.** Quantitative gene expression of TGF-β1, IL-10, TNF-α, and Fas ligand in renal cortex and medulla. *Nephrol Dial Transplant* 17: 573–579, 2002.
55. **Wang R, Ramos C, Joshi I, Zagariya A, Pardo A, Selman M, and Uhal B.** Human lung myofibroblast-derived inducers of alveolar epithelial apoptosis identified as angiotensin peptides. *Am J Physiol Lung Cell Mol Physiol* 277: L1158–L1164, 1999.
56. **Wells GM, Catlin G, Cossins JA, Mangan M, Ward GA, Miller KM, and Clements JM.** Quantitation of matrix metalloproteinases in cultured rat astrocytes using the polymerase chain reaction with a multi-competitor cDNA standard. *Glia* 18: 332–340, 1996.
57. **Woessner JF.** The determination of hydroxyproline in tissue and protein samples containing small proportions of this amino acid. *Arch Biochem Biophys* 93: 440–447, 1961.
58. **Woessner JF and Nagase H.** *Matrix metalloproteinases and TIMPs*. New York: Oxford Univ. Press, 2000.
59. **Yaguchi T, Fukuda Y, Ishizaki M, and Yamanaka N.** Immunohistochemical and gelatin zymography studies for matrix metalloproteinases in bleomycin-induced pulmonary fibrosis. *Pathol Int* 48: 954–963, 1998.
60. **Yu Q and Stamenkovic I.** Cell surface-localized matrix metalloproteinase-9 proteolytically activates TGF-β and promotes tumor invasion and angiogenesis. *Genes Dev* 14: 163–176, 2000.